C.P. No. 1352

C.P. No. 1352

PROCUREMENT EXECUTIVE, MINISTRY OF DEFENCE

AERONAUTICAL RESEARCH COUNCIL

CURRENT PAPERS

Planar Incompressible Flow over an Aerofoil and its Wake

by

F. T. Smith

Aerodynamics Dept., R.A.E., Farnborough

LONDON: HER MAJESTY'S STATIONERY OFFICE

1976

£1-60 NET

UDC 533.6.011.32 : 533.692 : 533.6.048.3 : 532.526

*CP No.1352
November 1974

PLANAR INCOMPRESSIBLE FLOW OVER AN AEROFOIL AND ITS WAKE

by

F. T. Smith**

SUMMARY

The Report describes a method for obtaining the incompressible flow over a given two-dimensional aerofoil at incidence, in which the rigid body and its boundary layer and wake are considered as forming a single semi-infinite body past which the inviscid fluid flows. The objective is to enable the viscous effects to be accommodated directly into an inviscid calculation, particularly near the sharp trailing-edge, where the singular point is in reality smoothed over by the boundary layer, and in the thin wake, whose shape has to be determined. By a conformal mapping to a halfplane an iterative cycle is set up to compute the solution, each iteration starting with a given shape, from which velocities are found, and ending with a suitable new guess for the wake shape, subject to certain conditions on the pressure and slope discontinuities across the wake. Results are presented for a Karman-Trefftz section of medium camber, both in the inviscid limit of zero displacement thickness (in which there is very good agreement with the exact solution) and for small nonzero displacement thicknesses near the trailing edge and in the wake. The method should be applicable to further problems.

This work was done under the link between the University of Southampton and the RAE while the author was a research fellow at Southampton.

---

* Replaces RAE Technical Report 74169 - ARC 36115

** Department of Mathematics, Imperial College, London, SW7.

CONTENTS

1 INTRODUCTION

This Report is concerned with the classical problem of finding the two-dimensional fluid flow at high Reynolds number past a given aerofoil section. The development by Catherall, Foster and Sells[1] of a conformal mapping method for determining the inviscid incompressible motion about a finite aerofoil brought about a substantial advance in the field of inviscid flow calculations. Their numerical technique necessitates finding the transformation that takes the exterior of the given body to the exterior of a circle. It has subsequently been applied in the method of Sells[2] to solving compressible flows for sub-critical conditions and by Garabedian and his collaborators[3-6] to solving transonic motions including weak shocks, although to cope with the source and vortex singularities at infinity in the physical plane the map to the interior of a circle has proved to be more convenient.

The comparisons made by Foster[7] of various other methods in use, e.g. the surface-singularity treatment by Smith[8] and the Thwaites-Theodorsen[9,10] method, and the later comparisons by Catherall *et al.*[1], indicate that the basic Catherall-Foster-Sells technique is definitely the most successful to date. More recently, with a view to predicting transonic flows, a number of other methods[11-14] have evolved, while a quasi-linearized approach to the subcritical problem, developed by Firmin[15] with the eventual aim of application to three-dimensional motions, embodies an appreciation of the viscous effects similar to that in Powell's[16] scheme, but incorporating an improved treatment of the wake.

Apart from the difficulties encountered in computing realistic transonic solutions, perhaps the most serious drawback in many current procedures lies in the treatment of the interaction between the inviscid pressure distribution and the viscous effects. As yet the process of incorporating in the inviscid calculation the influence of the viscous layers, on and behind the aerofoil, has not been possible in a wholly consistent or direct way. Usually the inviscid flow is first calculated, the displacement thicknesses are then derived for the boundary layer subject to the inviscid pressure distribution along the body, and these are fed back into the original inviscid scheme to produce a corrected, effective, body shape. However, this cycle automatically involves considerable difficulties. For example, if the trailing edge is sharp the Kutta-Joukowski condition, requiring a zero velocity there, produces an associated sharp adverse pressure gradient which then causes the boundary layer calculation to break down and can even provoke an unrealistic separation, unless some intuitive smoothing

is performed locally. Moreover, at the third stage of the cycle outlined above, the body with its displacement thickness forms a shape of infinite extent whereas nearly all the present accurate inviscid programs can be used only for finite bodies, necessitating a cutting off of the wake at an arbitrary point downstream.

In an attempt to provide a more satisfactory description of the actual airflow, a method is here developed for calculating the inviscid incompressible flow over the effective shape consisting of the original rigid body plus its viscous layers. Alternatively, this approach may be considered for the third stage of the cycle detailed in the previous paragraph - this aspect is expounded in section 5. In reality a sharp or cusped trailing edge is smoothed over locally by the viscous boundary layer and downstream the wake is of finite thickness. These features are incorporated directly by commencing with an estimate of the combined shape and, to solve for the resultant flow, the exterior of this shape is mapped conformally to an upper halfplane. The cusping effect of the (thin) viscous layer at the rear end of the aerofoil is accounted for by moving the singularity creating the stagnation point just inside the effective body (although the conventional inviscid problem of zero displacement thickness can also be dealt with as a special case). The problem thus set reduces to computing, by an iterative process, the modulus of the transformation; and the shape of the wake, upon which certain criteria on the jumps in slope and pressure are enforced, also comes out in the course of the calculations. In fact the method of derivation of the wake shape, step-by-step, forms a most significant part of the routine (see sections 2.4 and 3.4). For zero displacement thickness the method is 'exact' in the numerical sense, while for nonzero displacement thickness there are a number of free parameters whose values depend on the assumed boundary-layer calculation. The further possibilities of adding a fast intermediate viscous calculation, to confirm the displacement thickness, and/or of extending the work to compressible conditions, are discussed.

2 THE BASIC CONCEPT

By including, right from the start, a boundary layer on the given profile and also a wake downstream, the task of determining the incompressible flow over the finite aerofoil (and in particular calculating the pressure coefficient on the surface) is recast into the problem of finding the flow past the semi-infinite body that comprises both the aerofoil and the induced viscous layers.

The shape and size of the boundary layer and wake must be considered unknown, although assuming no large-scale separation occurs it is reasonable to suppose them to be relatively thin. Incorporating the displacement surface does of course introduce some difficulties inherent in dealing with an infinitely long body, but these are largely offset by the number of advantages to our approach. For the new combined profile now contains no sharp corners or cusped points, in contrast with the usual aerofoils considered; a sharp trailing-edge, for instance, is replaced by the smooth layer of boundary layer thickness sweeping past it. Further, the inclusion of the displacement effect, especially at the trailing edge, is certainly more sensible on purely physical grounds than the Kutta-Joukowski condition hatitually applied there. Finally, there is much simplification in the mathematics involved in the conformal mapping routine employed to solve the central fluid motion problem, and this we now set out to describe.

2.1 Conformal mapping to a halfplane

The given body, which is smooth except for a sharp rear edge (the analysis is easily modified to treat a cusped edge) of angle d, is supposed fixed in a fluid that far upstream is moving with a uniform velocity U, at an angle α to the axis Ox of a cartesian coordinate system, $Oxy(z = x + iy)$. The domain exterior to the combined profile (given body + viscous layers) in the physical- or z-plane is mapped conformally to the upper half of the Z-plane in such a way that the whole profile corresponds to the real axis of Z, as depicted in Fig.1. The trailing streamline acts as a cut in the z-plane, and the map is so chosen that the upper and lower sides of the wake are taken to the intervals $X > 1$ and $X < -1$, respectively, of the X-axis, where $Z = X + iY$, while the remaining shape defined by the original body plus its boundary layer maps to the zone $-1 \leqslant X \leqslant 1$ of $Y = 0$.

If we write the complex potential for the flow in either plane as F, then the complex velocities in the physical plane and working (Z-) plane are given by

$$\frac{dF}{dz} = qe^{-i\theta}, \qquad \frac{dF}{dZ} = q_c e^{-i\theta_c} \tag{2-1}$$

in turn, with q denoting the speed and θ the flow inclination at any point of the z-plane, and correspondingly for q_c, θ_c in the Z-plane. The two velocity vectors are therefore related by

$$qe^{-i\theta} = q_c e^{-i\theta_c} \left(\frac{dZ}{dz}\right) \quad . \tag{2-2}$$

Since the map $z \to Z$ is conformal $\left(\frac{dz}{dZ}\right)$ is nonzero in $\mathrm{Im}Z \geq 0$, and provided the front stagnation point on the effective body - this is the sole remaining stagnation point outside or on the body - in the z-plane transforms exactly to a stagnation point in the Z-plane (in fact, on the X-axis), we may then take logarithms of both sides in (2-2). Hence

$$\ln\left(\frac{dz}{dZ}\right) = \ln\left(\frac{q_c}{q}\right) + i(\theta - \theta_c) \tag{2-3}$$

is a function of Z analytic in the upper halfplane, with

$$h = \ln(q_c/q) \ , \qquad \phi = (\theta - \theta_c) \tag{2-4}$$

its real and imaginary parts respectively. From complex variable theory it follows that, if one of the functions h, ϕ is known, the other is determined uniquely to within an arbitrary constant, and the idea now is to express their relationship in a closed, integral, form (see section 2-2).

Before doing this, however, it is necessary to consider the incompressible flow in the Z-plane that we are looking for. It must merely have a stagnation point somewhere along the real axis and, by analogy with the map $z_1 = Z^2$ which transforms the whole z_1-plane with a cut along $y_1 = 0$, $x_1 > 0$ into the upper half of the Z-plane, its complex potential must behave like a constant multiple of Z^2 at infinity. Suitably normalized, the required solution is

$$F(Z) = \tfrac{1}{2}AZ^2 + BZ \tag{2-5}$$

implying $q_c e^{-i\theta_c} = AZ + B$. Here A and B are real constants, so that the one stagnation point is on the real axis at $X = -B/A$. On the effective profile, i.e. along the X-axis, $q_c = |AX + B|$ and θ_c is zero to the right of $X = -B/A$ and $-\pi$ to the left. We observe that in our notation θ also jumps by $-\pi$ as we pass through the front stagnation point in the direction Q to P on the body, making ϕ continuous at $X = -B/A$, and it proves to be expedient to *re-define* θ, θ_c, q and q_c at this juncture. Along the X-axis we now add π to the above values of θ and θ_c for all $X < -B/A$ and

simultaneously make q and q_c change sign in $X < -B/A$. The definitions throughout the flow field are altered likewise, and this has the advantage of rendering q, q_c, θ and θ_c, as well as h and ϕ, continuous for all X. Also, on the body, which is itself a streamline, $\theta(s)$ can now be specified as the continuous profile slope, without prior knowledge of A or B; e.g. for a symmetrical profile, $\theta(s)$ changes continuously along the upper surface from the value $-d/2$ at the trailing edge to $\pi/2$ at the leading edge and then, on the lower surface, from $\pi/2$ to $(\pi + d/2)$ at the trailing edge. The functions h and ϕ are unaltered by these definitions, but now, on $Y = 0$,

$$q_c = AX + B , \qquad \theta = 0 \text{ for all } X . \tag{2-6}$$

If s measures distances along this body from some fixed origin then, on putting $Y = 0$ in the real part of (2-2) and in (2-4),

$$\frac{ds}{dX} = \frac{AX + B}{q(X)} = e^{h(X)} . \tag{2-7}$$

The other stagnation point in the z-plane, which by the Kutta-Joukowski condition is associated with the sharp rear edge T of the rigid aerofoil, has been supposed smoothed over by the boundary layer at the trailing edge (see Fig.1) and so lies between the upper and lower streamlines of the combined shape near T. Unlike the front stagnation point, it does not appear in the flow in the Z-plane (2-5) but rather in the map function $z \to Z$. When the conformal mapping is applied, the actual trailing edge point T is transformed into two points in the Z-plane situated immediately below the real axis at $X = \pm 1$ where the body region joins the wake region. Specifically, we therefore require

$$q = 0 \text{ at } \begin{cases} X = 1 - i\varepsilon_1 & (T' \text{ in Fig.1}) \\ X = -1 - i\varepsilon_2 & (T'') \end{cases} \tag{2-8}$$

where the unknown parameters ε_1, ε_2 are non-negative and, assuming the viscous layer near T is thin, are relatively small. Thus the Kutta-Joukowski condition has been replaced by the more realistic requirement that a stagnation point should be present at a small distance inside the effective body surface (although $\varepsilon_1 = \varepsilon_2 = 0$ can be taken as a special case - see section 4).

2.2 The h-ϕ relationship

Considering now the relationship existing between h and ϕ, the analytic function $(h + i\phi) \equiv \ln\left(\frac{dz}{dZ}\right)$ is slightly inappropriate to deal with as it stands because

(i) from (2-3) and since $|q| \to U$ as $|z| \to \infty$, $(h + i\phi)$ grows like $\ln\{(AZ + B)/U\} + i\alpha + O(1)$ as $|Z| \to \infty$

(ii) from (2-4), (2-8) and using the modulus of (2-5) for q_c, $(h + i\phi)$ has a logarithmic singularity at T' and T''.

It is preferable to consider a related function analytic in $\mathrm{Im}Z \geq 0$ that is bounded at infinity and further, from the computational standpoint, this function should be free of singularities at T', T'' or anywhere within a close neighbourhood of the boundary $Y = 0$ of our zone of interest. For otherwise, even though $\ln(dz/dZ)$ is mathematically well-behaved on the real axis near $X = \pm 1$, in practice the existence of the two singular points at small distances ε_1, ε_2 below the axis would considerably distort the numerical accuracy there.

To accomplish these requirements the irregular behaviour in $(h + i\phi)$ is subtracted out, a procedure equivalent to performing an intermediate mapping as done by Catherall *et al.*[1]. For (i) the function $[\ln\{(AZ + B)/U + i\} + i\alpha]$ eliminates the growth at infinity without bringing in any other irregularities in $\mathrm{Im}Z \geq 0$. To accommodate (ii) we need an expression for the behaviour of $(h + i\phi)$ around T' and T'', and for this purpose the rear end of the profile (Fig.2) may be viewed locally as a sharp corner, for which the map to a half-plane is well-known. We thereby find that, since ε_1 and ε_2 are small,

$$h + i\phi \approx \begin{cases} -\frac{d_1}{\pi} \ln(Z - 1 + i\varepsilon_1) + O(1) & \text{near } T' \\ -\frac{d_2}{\pi} \ln(Z + 1 + i\varepsilon_2) + O(1) & \text{near } T'' \end{cases} \qquad (2\text{-}9)$$

The unknown angles d_1, d_2, satisfying $d_1 + d_2 = d$, are defined in Fig.2, and (2-9) allows for the singularities in (dz/dZ) near $Z = \pm 1$ as required, in that along the trailing streamline $\arg(dz/dZ)$ jumps by $-d_1$ at P' and by $-d_2$ at Q'. Hence in the vicinity of $X = \pm 1$, $Y = 0$ the term

$$- \frac{d_1}{\pi} \ln (Z - 1 + i\varepsilon_1) - \frac{d_2}{\pi} \ln (Z + 1 + i\varepsilon_2) \qquad (2\text{-}10)$$

should be removed from $(h + i\phi)$. At the same time, rather than introduce the growth (2-10) for $|Z| \gg 1$, another term, $-(d/\pi) \ln (Z + i)$, is included, which cancels with (2-10) as $|Z| \to \infty$ since $d = d_1 + d_2$ and leaves a singularity only at $Z = - i$, a satisfactory distance (in the numerical sense) away from the flowfield $\mathrm{Im}Z \geq 0$.

Summarizing, the new function

$$(H + i\Phi)(Z) \equiv (h + i\phi) - \left\{ \ln \left(\frac{AZ + B}{U} + i \right) + i\alpha \right\} + \frac{d_1}{\pi} \ln (Z - 1 + i\varepsilon_1) + \frac{d_2}{\pi} \ln (Z + 1 + i\varepsilon_2) - \frac{d}{\pi} \ln (Z + i) \qquad (2\text{-}11)$$

has the desirable properties that it is analytic everywhere in $\mathrm{Im}Z \geq 0$ and within small distances of the real axis, and tends to zero as $|Z| \to \infty$ in $\mathrm{Im}Z \geq 0$. Stemming directly from this are the following relationships between the real and imaginary parts $H(X)$, $\Phi(X)$, the values of H, Φ on $Y = 0$:

$$H(X) = - \frac{1}{\pi} \fint_{-\infty}^{\infty} \frac{\Phi(\xi) d\xi}{X - \xi} \qquad (2\text{-}12a)$$

$$\Phi(X) = \frac{1}{\pi} \fint_{-\infty}^{\infty} \frac{H(\xi) d\xi}{X - \xi} \qquad (2\text{-}12b)$$

which may be arrived at by application of Cauchy's integral formula or by Fourier transform techniques (Carrier, Krook and Pearson[17]). Here $\fint$ denotes the principal value of an integral, and from (2-6) and (2-11), with $Z = X$, $H(X)$ and $\Phi(X)$ may be written down explicitly as

$$H(X) = \ln \left(\frac{q_c}{q} \right) + \frac{d_1}{2\pi} \ln \left[\frac{(X - 1)^2 + \varepsilon_1^2}{X^2 + 1} \right] + \frac{d_2}{2\pi} \ln \left[\frac{(X + 1)^2 + \varepsilon_2^2}{X^2 + 1} \right] - \frac{1}{2} \ln \left[\left(\frac{AX + B}{U} \right)^2 + 1 \right] \qquad (2\text{-}13a)$$

$$\Phi(X) = \theta(X) - \alpha + \frac{d_1}{\pi}\tan^{-1}\left(\frac{\varepsilon_1}{X-1}\right) + \frac{d_2}{\pi}\tan^{-1}\left(\frac{\varepsilon_2}{X+1}\right) - \frac{d}{\pi}\tan^{-1}\left(\frac{1}{X}\right) - \tan^{-1}\left(\frac{U}{AX+B}\right) \qquad (2\text{-}13b)$$

with h and ϕ substituted from (2-4). For definiteness we have taken $0 \leqslant \tan^{-1} < \pi$ in (2-13b).

2.3 Determination of A and B

The constant A is simply a stretching factor ensuring that the difference $[s(X = 1) - s(X = -1)]$ is exactly the distance round the effective aerofoil, from P to Q, and is quite easily calculated (see section 3.2). The determination of B is somewhat more involved and relies on the asymptotic result, for $|X| \to \infty$,

$$H(X) = \left(\frac{d_2 - d_1}{\pi X}\right) + \frac{1}{2\pi X^2}\left(d_1\varepsilon_1^2 + d_2\varepsilon_2^2 - 2d - \frac{\pi U^2}{A^2}\right) + o(X^{-2}) \qquad (2\text{-}14)$$

proved in Appendix A. But alternatively (2-12a) implies, on taking care over the principal value involved and knowing the asymptotic form of $\Phi(X)$ (see Appendix A), that

$$H(X) \sim -\frac{1}{\pi X}\int_{-\infty}^{\infty} \Phi(\xi)d\xi \qquad \text{for } |X| \gg 1$$

and so (2-14) places on $\Phi(X)$ the requirement

$$\int_{-\infty}^{\infty} \Phi(X)dX = (d_1 - d_2) \quad . \qquad (2\text{-}15)$$

Inserting the definition of Φ, in (2-13b), into (2-15) and integrating the inverse tangent terms, we deduce the formula

$$-\pi\frac{B}{A} = \int_0^{\infty} [\theta(X) - \alpha]dX + \int_{-\infty}^{0} [\theta(X) - \pi - \alpha]dx \quad . \qquad (2\text{-}16)$$

For known shape of body and wake, (2-16) fixes B. It is noteworthy that, for a symmetrical aerofoil at zero incidence, $B = 0$ and the solution is completely symmetrical about the Y-axis, as we should expect.

2.4 The mixed boundary conditions

Finally in this section we observe that, because of the essential difference between the flow problem over the body and that in the wake, both (2-12a) and (2-12b) are of importance in the solution. If the function $s(X)$, the principal unknown, were given, then on the body, $|X| \leq 1$, since the shape $\theta(s)$ is prescribed, $\Phi(X)$ is known (from (2-13b)) so that (2-12a), relating $H(X)$ and hence $q(X)$ to $\Phi(X)$, is the relevant integral relation. In the wake part, $|X| > 1$, on the other hand, both $\theta(s)$ and $q(s)$ are unknown - what can be prescribed are two sets of jump conditions (see sections 3.1 and 3.4) on the θ, q values either side of the wake, each set constituting a 'half-condition'. Thus the solution in $|X| > 1$ calls for the use of the alternative integral formula (2-12b), as well as (2-12a), to allow the wake to develop towards its correct shape. The way this was done in practice is described in section 3.4 below.

3 THE NUMERICAL SCHEME

3.1 Formulating the problem

The process of mapping to the halfplane as set out in section 2.1 is in principle remarkably simple. A major task now is to decide which quantities are given, and which are to be found, during the calculation routine, and in this connection it is necessary to stress the two fundamental ways in which our method could be of use. The first is as an extension of the existing methods for obtaining the inviscid flow and (then) the associated boundary layer thickness. Here the present work should increase their combined accuracy by determining the flow past the known body together with its quite precisely calculated displacement surface. Secondly, the method may be used *ab initio* (and with ε_1, ε_2 zero or nonzero) as a direct alternative to the existing inviscid-flow numerical schemes, and it is this situation, where the displacement surface is not yet known, that we shall subsequently be concerned with in the main.

It is supposed therefore that the basic profile is specified in terms of its (x,y) coordinates and that U, d and α are prescribed. Additionally, (s,θ) values are set to describe an initial guess for the wake shape, an unknown,

and the (x,y) values are then converted (see below) to produce a reference table of (s,θ) coordinates defined as in section 2.1. For convenience, the total distance round the profile from P to Q is written as $2s_0$ and the origin s is selected such that

$$s(P) = -s_0 , \qquad s(Q) = s_0 . \tag{3-1}$$

So far we have in practice neglected the viscous displacement on the rigid profile, i.e. in $|X| \leqslant 1$, save near the trailing edge T where it is of course crucial, for the local calculation at least, to consider a displacement of the stagnation point inside the effective body. Either side of T the profile is therefore joined smoothly to the wake by fixing appropriate values for θ at P, Q and just upstream. The wake is not necessarily made to fare into a single streamline aft of the body; rather, a thin wake of uniform thickness is allowed to develop downstream (see section 3.4), as a physically reasonable first approximation, when ε_1 and ε_2 are nonzero.

Thus in our formulation we commence with a known body profile $\theta(s)$ in $|s| \leqslant s_0$ and a first guess for the wake shape $\theta(s)$ in $|s| > s_0$. Small values for ε_1, ε_2 are set to allow for the boundary layer thickness near T (at $X = \pm 1$), the thickness being controlled by ε_1 and ε_2 and being zero if and only if ε_1 and ε_2 are zero (see section 4). The objective is to determine $q(s)$, the wake shape $\theta(s)$ and the displacement near the trailing edge for given ε_1 and ε_2.

The eventual solution for the wake shape has so far been made to satisfy the criteria that at corresponding points on either side of the trailing streamline the flow speeds and directions must be the same. This means that, if supercripts $\pm$ refer to values on the upper and lower surfaces respectively, then we insist that $q^+ = -q^-$, $\theta^+ = \theta^- - \pi$ when $s^+ = -s^-$ for $|s| > s_0$. Provided the forces due to wake curvature are fairly negligible (*cf.* Firmin[15]), the condition on q is equivalent to the requirement of no transverse force on the wake, while that on θ likewise neglects viscous effects within the wake. In fact the inclusion of the proper viscous corrections would not be too difficult a step.

Applying the $q^+ = -q^-$ condition at $X = \pm 1$ (i.e. at P and Q in Fig.2) would yield ε_2 in terms of ε_1 at any stage, but in general both ε_1 and ε_2 have been kept as free parameters because it is not entirely clear if

the condition is appropriate near the trailing edge. Further discussion is presented in section 5.

3.2 The iterative routine for solution

The problem posed is of a mixed boundary-value type and is solved numerically by an iterative scheme. Letting $^{(n)}$ signify nth approximations, the logic consists of the following consecutive steps, executed until successive iterates are sufficiently close in value.

(1) Given $\theta(s)$ in $|s| \leqslant s_0$, guess $\theta(s)$ in $|s| > s_0$ and $s^{(1)}(X)$ for all X. Put $A^{(1)} = 2s_0$, $d_1^{(1)} = d_2^{(1)} = d/2$. Set $n = 2$ and go to (4).

(2) Integrate (2-7) to obtain $s^{(n)}(X)$, starting from $s^{(n)}(-1) = -s_0$, and scale A, B to make $s^{(n)}(1) = s_0$.

(3) Derive $\theta^{(n)}(X)$ by interpolation in the θ-s reference table to find the value $\theta^{(n)}$ corresponding to each $s^{(n)}$.

(4) Calculate $B^{(n)}$ from (2-16) and hence $\Phi^{(n)}(X)$ from (2-13b).

(5) Use (2-12a) to evaluate $H^{(n)}(X)$, and then (2-13a) to give a new distribution $q^{(n)}(X)$.

(6) Revise the wake part of the reference table, $\theta^{\pm}(s)$, to keep the $q^{\pm}$ condition satisfied, and calculate $d_1^{(n)}$, $d_2^{(n)}$, as explained in section 3.4 below. Increase n by 1, return to (2) and continue.

3.3 Finer points of the calculations

In discretizing the method, a large number M of points $X_i (1 \leqslant i \leqslant M)$ is laid down on the X-axis at small equal intervals $(X_{i+1} - X_i) = \Delta$. Two of these points coincide with $X = \pm 1$, say $X_J = -1$, $X_K = 1$, and $(K - J + 1)$ is usually the number of profile points specified or a multiple thereof, while for symmetry we set $M - K + 1 = J$. Therefore $X_N = 0$ where $2N = K + J$. The subscript i describes values at $X = X_i$.

The guesses in step (1) above should be sensible, in that the $\theta^{\pm}$ conditions are obeyed, and we initially place θ^+, $(\theta^- - \pi)$ equal to α and q^+, $-q^-$ equal to U at the extreme ends $i = 1$, $i = M$. If the program is not supplied with aerofoil coordinates in (s,θ) form, but with (x,y) data, these are converted using Freeland's[18] cubic spline fit scheme and, if necessary, parabolic smoothing (see Catherall *et al.*[1]) near the leading edge,

to produce a good representation of the aerofoil's slope. To give an initial guess, $s^{(1)}(X)$, for the s_i values, the values of s in the θ-s reference table are taken.

At stage (2) it is safe to integrate the ratio $(AX + B)/q$ in (2-7) straightforwardly, starting with $s_J = -s_0$ and marching forwards or backwards with the two-point formula

$$s_i - s_{i-1} = \frac{\Delta}{2}\left(\frac{AX_i + B}{q_i} + \frac{AX_{i-1} + B}{q_{i-1}}\right) \qquad (3\text{-}2)$$

except through the troublesome points $X = \pm 1$, $X = -B/A$. Now q is always defined by

$$q(X) = (AX + B)e^{-H(X)} \frac{\left[(X-1)^2 + \varepsilon_1^2\right]^{d_1/2\pi} \left[(X+1)^2 + \varepsilon_2^2\right]^{d_2/2\pi}}{(1+X^2)^{d/2\pi}\left[\left(\frac{AX+B}{U}\right)^2 + 1\right]^{\frac{1}{2}}} \qquad (3\text{-}3)$$

where all the factors excluding $(AX + B)$ are nonzero and well-behaved for $\varepsilon_1, \varepsilon_2 > 0$. Hence (2-7) can easily be taken through $X = -B/A$, either by cancelling the factors $(AX + B)$ in formulae (2-7) and (3-3) or by forming $(ds/dX)(X = -B/A) = A\Big/\left(\frac{dq}{dX}\right)(X = -B/A)$ and interpolating between points either side of the stagnation point. The other difficulties, at $X = \pm 1$, are due to the (integrable) singularities at $X = 1 - i\varepsilon_1$, $X = -1 - i\varepsilon_2$ which, as in section 2.2, could upset the local calculations even for nonzero ε_1, ε_2 if no special treatment were employed; moreover we wish to be free to set the special case $\varepsilon_1 = \varepsilon_2 = 0$ that recovers the conventional Kutta-Joukowski condition. Consequently a localised allowance is made for the erratic behaviour by replacing (3-2) with

$$s_i - s_{i-1} = \left[e^H \frac{(1+X^2)^{d/2\pi}}{\left\{(X+1)^2 + \varepsilon_2^2\right\}^{d_2/2\pi}} \left\{\left(\frac{AX+B}{U}\right)^2 + 1\right\}^{\frac{1}{2}} \right]_{i-\frac{1}{2}} \int_{X_i}^{X_i+\Delta} \frac{d\xi}{\left[(\xi-1)^2 + \varepsilon_1^2\right]^{d_1/2\pi}} \qquad (3\text{-}4)$$

for $i = J, J-1$ and similarly at $i = K-1, K$. The integral here is

$$I = \int_0^1 \frac{dt}{\left(t^2 + \frac{\varepsilon_1^2}{\Delta^2}\right)^{d_1/2\pi}} \Delta^{1-d_1/\pi} \qquad (3\text{-}5)$$

and is evaluated numerically using a trapezoided rule if $\varepsilon_1 \neq 0$. When $\varepsilon_1 = 0$, $I = \Delta^{1-d_1/\pi} \Big/ (1 - d_1/\pi)$.

Having obtained $s_i^{(n)}$ values for $1 \leqslant i \leqslant M$, with $s_J^{(n)} = -s_0$, a new result $A^{(n)}$ is determined by

$$A^{(n)} = \hat{f} A^{(n-1)} \quad \text{where} \quad \hat{f} = \left(\frac{2s_0}{s_K^{(n)} + s_0}\right) . \qquad (3\text{-}6)$$

The linearity of this transformation arises from the integration of $(AX + B)/q$ with the known q-values or alternatively by inserting (3-3) into (2-7). Multiplying B by the same factor $\hat{f}$ and scaling the $s_i^{(n)}$ in accord:

$$s_i^{(n)} - s_J^{(n)} \rightarrow \hat{f}\left(s_i^{(n)} - s_J^{(n)}\right) \qquad (3\text{-}7)$$

we comply with the constraint $s_K^{(n)} = s_0$ as well as retaining (2-7).

To find the $\theta_i^{(n)}$ corresponding to the $s_i^{(n)}$ values (step (3)) a two-point method similar to that of Catherall *et al.*[1] is adopted. If $s_i^{(n)}$ lies between the values s_{i_1}, s_{i_1+1} of the original θ-s table the value is written as the appropriate linear interpolation between θ_{i_1}, θ_{i_1+1}. We note that the re-definition of the θ's made in section 2.1 greatly facilitates this step.

In proceeding from stage (2), and in stage (3), an under-relaxation procedure is adopted. Instead of the $s_i^{(n)}$ evaluated in stage (2) the linear combinations $\bar{s}_i^{(n)} = w s_i^{(n)} + (1 - w)\bar{s}_i^{(n-1)}$ are taken as the new s-values. Next, for the new θ's we then take $\bar{\theta}_i^{(n)} = \ell\theta_i^{(n)} + (1 - \ell)\bar{\theta}_i^{(n-1)}$ for $J \leqslant i \leqslant K$,

the $\theta_i^{(n)}$ here being the values obtained as in the previous paragraph. Initially $\bar{s}_i^{(1)}$, $\bar{\theta}_i^{(1)}$ are put equal to the numbers in the θ-s table. The relaxation parameters w, ℓ were vital to the success of the scheme for, when $w = 1$ and/or $\ell = 1$ were imposed, convergence was not obtained. w and ℓ were usually set equal to 0.5 at the outset and halved after a few iterations, and this gave reasonably fast convergence. Relaxation was not applied to the θ_i in the wake part for reasons given in section 3.4 below.

The calculation of $B^{(n)}$ at step (4) employs the trapezium rule applied to the integral between $X_1 (= -R$, say) and $X_M (= R)$, but to increase the accuracy the approximate contribution from the integrand beyond $|X| = R$ is brought in, involving the asymptotic forms

$$\left.\begin{matrix} \theta^+(X) - \alpha \\ \theta^-(X) - \pi - \alpha \end{matrix}\right\} \sim \frac{-\Gamma}{\pi A X^2} + o(X^{-2}) \qquad \text{for } |X| \to \infty \qquad (3\text{-}8)$$

(see Appendix A) and inserting them into (2-16) for $|X| > R$. Since Γ, the circulation round the aerofoil, is 2B, the resultant discrete version of (2-16) is

$$-\pi \frac{B^{(n)}}{A^{(n)}} \left(1 - \frac{4}{\pi^2 R}\right) = \Delta \sum_{i=N}^{M-1} \left(\tfrac{1}{2}\theta_i^{(n)} + \tfrac{1}{2}\theta_{i+1}^{(n)} - \alpha\right) + \Delta \sum_{i=1}^{N-1} \left(\tfrac{1}{2}\theta_i^{(n)} + \tfrac{1}{2}\theta_{i+1}^{(n)} - \pi - \alpha\right) .$$

.....(3-9)

The $\Phi_i^{(n)}$ then follow from (2-13b), taking suitable action, particularly at P', Q' and near $X = -B/A$, to keep $0 \leqslant \tan^{-1} \leqslant \pi$.

In step (5) the $H_i^{(n)}$ are also worked out from the trapezium rule applied for $|\xi| \leqslant R$ in (2-12a) and again the finite extent of the integration range is corrected for by including the asymptotic contribution from $|\xi| > R$. Initially therefore,

$$H_i^{(n)} = \sum_{\substack{j=1 \\ (j \neq i, i-1)}}^{M-1} \left\{ \frac{\Phi_j^{(n)}}{(j - i)} + \frac{\Phi_{j+1}^{(n)}}{(j + 1 - i)} \right\} \frac{1}{2\pi} + \left(\frac{\Phi_{i+1}^{(n)} - \Phi_{i-1}^{(n)}}{\pi} \right) \qquad (3\text{-}10)$$

is evaluated for $2 \leq i \leq M - 1$ to give a second-order accurate principal value of the integral from $-R$ to R, incorporating a consistent Taylor expansion around $j = i$. Next, we add to each $H_i^{(n)}$ of (3-10) the value of

$$\frac{2B}{\pi^2 A}\left\{\frac{1}{X^2}\ln\frac{R-X}{R+X}+\frac{2}{RX}\right\}-\frac{d_1\varepsilon_1}{\pi^2(X-1)}\ln\left(\frac{R+1}{R-1}\frac{R-X}{R+X}\right)-\frac{d_2\varepsilon_2}{\pi^2(X+1)}\ln\left(\frac{R-1}{R+1}\frac{R-X}{R+X}\right)$$
$$+\frac{d}{\pi^2 X}\ln\left(\frac{R-X}{R+X}\right)-\frac{U}{\pi(AX+B)}\ln\left(\frac{R+B/A}{R-B/A}\frac{R+X}{R-X}\right) \qquad (3\text{-}11)$$

at $X = X_i$, except at P', Q' and near $X = -B/A$ where limiting values in (3-11) must be substituted. The leading term in (3-11) comes from the asymptotic form (3-8) of the $(\theta - \alpha)$ term of (2-13b) and then insertion into (2-12a) for $|\xi| > R$, while the other expressions in (3-11) are from the expansions, also accurate to $O(X^{-2})$, of the inverse tangents in (2-13b). The end conditions stipulated are $H_1^{(n)} = H_M^{(n)} = 0$. The corresponding variation of $q(X)$ follows immediately from (3-3).

3.4 Finding the shape of the wake

The final step in the iterative cycle is always reached with the $\theta^{\pm}$ condition satisfied but the $q^{\pm}$ one slightly awry. In other words, the wake is still thin but of the wrong shape. To compensate we revise the basic θ-s table in $|s| > s_0$ at each iteration, exploiting the relation (2-12b), the inverse of (2-12a), to deal with the mixed boundary-value nature of the problem. First, the q_i values (for $i < J$, $i > K$) are adjusted to make $q^+ = -q^-$ when $s^+ = -s^-$, which is achieved by means of an averaging process: for each $i < J$ we find s_{i_1-1}, s_{i_1}, $i_1 > K$, such that $s_{i_1-1} < -s_i < s_{i_1}$, then interpolate linearly between q_{i_1-1}, q_{i_1} to find the value q^+ corresponding approximately to q_i and reset q_i equal to the average of $-q^+$ and the original q_i. Thus we take, instead of q_i, the value

$$\bar{q}_i = \tfrac{1}{2}\left\{q_i + \frac{\left(s_i + s_{i_1}\right)q_{i_1-1} - \left(s_i + s_{i_1-1}\right)q_{i_1}}{\left(s_i - s_{i_1-1}\right)}\right\} \qquad (3\text{-}12a)$$

for all $i < J$. Similarly, each q_i for $i > K$ is subsequently replaced by the value

$$\bar{q}_i = \left\{\left(s_i + s_{i_1}\right)\bar{q}_{i_1+1} - \left(s_i + s_{i_1+1}\right)\bar{q}_{i_1}\right\} \Big/ \left(s_{i_1} - s_{i_1+1}\right) \qquad (3\text{-}12b)$$

where now $-s_{i_1+1} < s_i < -s_{i_1}$, and so the $q^{\pm}$ condition is arrived at, but with the formula (2-12b) usually being violated.

Secondly, therefore, with the new q_i values in the wake, we work backwards, calculating new H_i values in $|X| > 1$ using (2-13a), then deriving Φ_i in $|X| \geq 1$ from a trapezoidal interpretation of (2-12b), and hence obtain new $\theta_i^{\pm}$ values $(i < J,\ i > K)$ from (2-13b). Specifically the discretization used for (2-12b), $i \leqslant J,\ i \geqslant K$, is

$$\Phi_i = \sum_{\substack{j=1 \\ (j\neq i,i-1)}}^{M-1} \left\{\frac{H_j}{(i-j)} + \frac{H_{j+1}}{(i-j-1)}\right\} \frac{1}{2\pi} + \left(\frac{H_{i-1} - H_{i+1}}{\pi}\right)$$

$$+ \frac{(d_2 - d_1)}{\pi^2 X_i} \ln\left(\frac{R+X}{R-X}\right)_i + \frac{1}{2\pi^2}\left[d_1\varepsilon_1^2 + d_2\varepsilon_2^2 - 2d - \frac{U^2\pi}{A^2}\right] \times$$

$$\left[\frac{2}{RX_i} + \frac{1}{X_i^2} \ln\left(\frac{R-X}{R+X}\right)_i\right] \qquad (3\text{-}13)$$

which is an $O(\Delta^2)$ accurate integration between $X = \pm R$ followed by an allowance of the contributions from the integrand beyond $|X| = R$ arising from the asymptotic result (2-14) for the decay of $H(\xi)$ as $|\xi| \to \infty$.

Finally, an averaging technique is also performed on the new $\theta_i^{\pm}$ values, since the $\theta^{\pm}$ constraint will not in general be satisfied as the original wake thickness has now been disturbed. This again involves finding points of equal $|s|$ throughout $|X| > 1$ and then taking the mean value of the slopes there, using two-point interpolation; effectively, $\left(\theta_{i_1}^{+} - \pi\right)$ and θ_i^{-} replace $-q_{i_1}^{+}$, q_i^{-} respectively in (3-12a) and $\left(\theta_{i_1}^{-} + \pi\right)$ and θ_i^{+} replace $-q_{i_1}^{-}$, q_i^{+} respectively in (3-12b), and the $\theta^{\pm}$ condition is thereby reached. The values of θ, s in the reference table for $|s| > s_0$ now also take on the newly-calculated wake values, so that the basic θ-s table, although it is permanently fixed for the rigid body part $|s| \leqslant s_0$, is continually being updated in the wake $|s| > s_0$ by our program to keep in line with the constraints for a

well-defined wake. It is partly for this reason that relaxation is not applied in $|X| > 1$.

The angle d_1 is effectively the direction of the trailing streamline at the rear edge T and can now be evaluated from the Φ_J, Φ_K values derived in (3-13). Examination of the values of Φ at T' and T" , using (2-11) and (2-4) and with the limiting values for the inverse tangents there, gives, on averaging consistent with the previous paragraph,

$$
\begin{aligned}
d_1^{(n)} \left[1 + \frac{1}{2\pi} \left\{ \tan^{-1}\left(\frac{A\varepsilon_2}{A-B}\right) + \tan^{-1}\left(\frac{A\varepsilon_1}{A+B}\right) \right\} \right] &= \tfrac{1}{2}(\Phi_J + \Phi_K) - \frac{1}{4\Delta}\left[\varepsilon_1 (H_{K+1} - H_{K-1}) + \varepsilon_2 (H_{J+1} - H_{J-1})\right] \\
&\quad - \frac{1}{4\Delta^2}\left[\varepsilon_1^2 (\Phi_{K+1} - 2\Phi_K + \Phi_{K-1}) + \varepsilon_2^2 (\Phi_{J+1} - 2\Phi_J + \Phi_{J-1})\right] \\
&\quad - \hat{\theta}_K + \alpha + \tfrac{1}{2}\left[\tan^{-1}\left(\frac{A\varepsilon_1}{A+B}\right) - \tan^{-1}\left(\frac{A\varepsilon_2}{A-B}\right) + \tan^{-1}\left(\frac{U - A\varepsilon_1}{A+B}\right) - \tan^{-1}\left(\frac{U - A\varepsilon_2}{A-B}\right)\right] \\
&\quad + \frac{d}{2\pi}\left[\tan^{-1}\left(\frac{A\varepsilon_2}{A-B}\right) - \tan^{-1}\left(\frac{\varepsilon_2 - \varepsilon_1}{2}\right)\right] \qquad (3\text{-}14)
\end{aligned}
$$

to $O\left(\varepsilon_i^2\right)$, where $\hat{\theta}_K$ is the (known) inclination of the rigid profile's upper surface at T . If $\varepsilon_1 > \varepsilon_2$, $\tan^{-1}\left(\frac{\varepsilon_1 - \varepsilon_2}{2}\right)$ must be substituted for $-\tan^{-1}\left(\frac{\varepsilon_2 - \varepsilon_1}{2}\right)$ in (3-14). The angle $d_2^{(n)}$ is then equated to $\left(d - d_1^{(n)}\right)$.

4 EXAMPLES

The results presented here are all for the medium camber Karman-Trefftz profile (see Foster[7]), for which $d = 10^\circ$. In Fig.3a are shown the results obtained at $\alpha = 0^\circ$ in the classical limit of zero displacement thickness, $\varepsilon_1 = \varepsilon_2 = 0$. In this case most of the preceding analysis still applies on setting $\varepsilon_1 = \varepsilon_2 = 0$, but some care is needed in defining the inverse tangents, in evaluating B in (3-9) and especially in interpolating in the θ-s reference table which is now discontinuous at $s = \pm s_0$. The visual agreement between the known exact solution for the pressure coefficient and the calculated values is very good everywhere, and Fig.3b gives a close-up of the upper surface peak where the results are also compared with those of Catherall *et al.*[1] (the most accurate to date) and those of the Smith[8] singularity approach. The errors in

the present method are comparable with those of the calculations of Catherall *et al.* but are an order of magnitude smaller than Smith's[8]. Fig.3c depicts the solution for the wake shape.

For $\varepsilon_1 = \varepsilon_2 = 0$ the profile shape is known and the problem is well-posed. When ε_1 and ε_2 are nonzero, however, there are a number of free parameters present which, for their proper specification, would need to be determined from a viscous calculation near the profile and in the wake (see section 5). These parameters are ε_1, ε_2 and the effective profile shape upstream of P and Q. Without the viscous calculation, we have examined the behaviour of the solution for different values of ε_1 and ε_2 and for a given profile shape near T, in order to gauge the effects of the displacement, locally and globally, and the accuracy required of a boundary-layer calculation.

In Fig.4a are shown the solutions for the three sets of values $\varepsilon_i = 10^{-3}, 10^{-4}, 10^{-5}$ $(i = 1,2)$ together with the exact solution (for $\varepsilon_i = 0$) for the Karman-Trefftz section at $\alpha = 0^o$. The typical smoothing performed near T made θ_K equal to $(\hat{\theta}_K + d/4)$ ($\hat{\theta}_K$ is defined at the end of section 3.4) and θ_J equal to $(\hat{\theta}_J - d/4)$, with the four θ-values just upstream on each surface $(K - 1 \to K - 4,\ J + 1 \to J + 4)$ interpolated linearly from the profile to θ_K, θ_J respectively. The influence of the values of ε_1, ε_2 is almost negligible over most of the profile but quite pronounced near $|s| = s_0$, as might be expected. The trailing-edge area is shown in more detail in Fig.4b to emphasize the local differences in the solutions and results for $\varepsilon_i = 10^{-2}$ and for $\varepsilon_1 = 5 \times 10^{-3}$, $\varepsilon_2 = 10^{-3}$, both of which produce a quite smooth transition of C_p past the trailing-edge, are also included. Fig.4c is another close-up of the upper surface peak, demonstrating the relatively small overall effect of changes in ε_1 and ε_2. This was also demonstrated by the close agreement in the lift coefficients C_L. The C_L values were evaluated from the solutions for $q(s)$ but, as a check, C_L should be equal to twice the circulation (see, e.g. Sells[2]), or $4B$ in our treatment, and this was found to hold true to within 1% of C_L for each set of ε_i values. With ε_1 kept equal to ε_2 the lift increased steadily with increasing ε_i, varying from 1.23 at $\varepsilon_i = 0$ to 1.26 at $\varepsilon_i = 10^{-2}$. With the value of the displacement on the upper surface set larger than that on the lower surface, which for the present airfoil at $\alpha = 0^o$ is probably a more realistic assumption, one would intuitively expect there to be a decrease in lift; in fact, because of the discrepancies (mentioned in the next paragraph) in profile shape near T, an increase in ε_1 from

10^{-3} to 5×10^{-3} with ε_2 kept fixed at 10^{-3} resulted in a slight increase, of about 1%, in lift coefficient and similarly for the upper surface pressure peak in Fig.4c.

In Fig.4d are sketched the wake and body shapes that resulted for $\varepsilon_i = 0$, $\varepsilon_i = 10^{-3}$ and $\varepsilon_1 = 5 \times 10^{-3}$, $\varepsilon_2 = 10^{-3}$. It is somewhat difficult to form precise conclusions about the profile shapes near T from the results alone, owing to the loss of closure[1] involved in the smoothing of the profile and to numerical errors, but this minor weakness can be eradicated by a local analysis of the solution near T, some details of which are given in section 5 below, equation (5-1). Also in Fig.4d, in order to bring the final computed profile for $\varepsilon_1 = \varepsilon_2 = 0$ into closed form at the trailing edge, some allowance has been made for this loss of clarity by subtracting off the error in closure.

For 10° incidence the calculated solutions for $\varepsilon_1 = \varepsilon_2 = 10^{-4}$ and $\varepsilon_1 = \varepsilon_2 = 0$ are presented in Fig.5a, with the exact analytic solution for $\varepsilon_i = 0$, and again the accuracy is generally very good. Near the upper surface peak there is some discrepancy although the probable cause was insufficient precision in the representation of the leading-edge zone of the section. It is noteworthy that the map to the halfplane naturally tends to create a denser grouping of points around the front stagnation point than elsewhere, so that usually use of the constant steplength Δ, rather than a refined mesh near the leading-edge, is accurate enough for good definition. The wake shape for $\alpha = 10^{\circ}$ is drawn in Fig.5b.

All the above predictions were obtained using 72 points to define the profile. With 36 points the accuracy was diminished although only by an amount comparable with the corresponding results of Catherall *et al.*[1]. Another possible source of error apart from mesh size is that due to simulating the range $(-\infty,\infty)$ by $(-R,R)$. The above results were calculated using only $R \approx 3$ which corresponded to about 6 chord lengths range in the physical plane and no graphically distinguishable effects have been found when $R = 2$ or $R = 4$ has been taken instead. Other sections tested have been the NACA 0012 and RAE 101 aerofoils but these have more well-behaved profiles than the above Karman-Trefftz aerofoil and excellent agreement was obtained.

The scheme, when programmed on the CDC 6400 computer at Imperial College, needed between 30000 and 40000 octal words and usually took about 30 iterations, and 700 seconds including compilation and output, to converge to within a tolerance of 10^{-4} in the s_i values.

5 FURTHER DISCUSSION

The method presented above for the solution of the incompressible flow-field is generally about as accurate as the circle-transformation method[1] for the conventional problem with zero displacement, but one advantage is that it also allows the thickening effect of the viscous layers, particularly near the trailing-edge and in the wake, to be accommodated in the solution, for example by choice of nonzero ε_1, ε_2 . Again, downstream of the rigid body suitable (e.g. wake) conditions can be imposed *right on* the displacement surface because the method treats the body, together with its wake and displacement thickness, as an infinitely long profile. Thus, if viscous wake corrections to the solution were desired they could easily be applied (as (small) jumps in flow inclination and pressure across the wake) on the effective surface, and similarly for such situations as a trailing jetstream where again the downstream conditions make the problem mixed in nature.

The shape and size of the rear-edge displacement are governed by the parameters ε_1, ε_2 and by the values of θ near T , and would presumably be best derived from a boundary layer calculation married to the present approach. If, for instance, a guess were made for ε_1, $\varepsilon_2 (\neq 0)$, the boundary layer could be integrated past T using the resultant inviscid pressure distribution ($C_p < 1$ at P, Q) and hence a new value for the displacement thickness reached. The procedure could than be repeated for a number of different values of ε_1, ε_2 , using the first sets of solutions as initial guesses to speed up the convergence, and the relationship between ε_i and the viscous displacement thickness thus desired. In fact if the condition $|q_J| = |q_K|$ is imposed, ε_2 is controlled by ε_1 since (3.3) implies, on neglecting terms of relative order ε^2 ,

$$\varepsilon_2 = \varepsilon_1^{d_1/d_2} e^{(H_J - H_K)\pi/d_2} \left\{ \frac{1 + \left(\frac{U}{A - B}\right)^2}{1 + \left(\frac{U}{A + B}\right)^2} \right\}^{\pi/2d_2} \times 2^{1 - d_1/d_2} .$$

Also, to the same accuracy, we may integrate the equation

$$\frac{dz}{dZ} = e^H e^{i\Phi} \left(\frac{AZ + B}{U} + i \right) e^{i\alpha} (Z + i)^{d/\pi} (Z - 1 + i\varepsilon_1)^{-d_1/\pi} (Z + 1 + i\varepsilon_2)^{-d_2/\pi}$$

between T' and Q' and between T'' and P' (where dZ = idY) to obtain the displacements |TQ|, |TP| explicitly:

$$\left.\begin{aligned} |TQ| &= e^{H_K}\left[\left(\frac{A+B}{U}\right)^2+1\right]^{\frac{1}{2}} 2^{d_1-d_2/2\pi}\,\varepsilon_1^{1-d_1/\pi}\Big/(1-d_1/\pi) \\ |TP| &= e^{H_J}\left[\left(\frac{A-B}{U}\right)^2+1\right]^{\frac{1}{2}} 2^{d_2-d_1/2\pi}\,\varepsilon_2^{1-d_2/\pi}\Big/(1-d_2/\pi) \quad . \end{aligned}\right\} \tag{5-1}$$

Judging from our results it does appear, however, that errors in the boundary-layer calculation near T can have little overall influence on the solution, provided they are not too large.

Concerning the other natural extension to attempt with our method, that of predicting compressible flows, some difficulty is envisaged because the modulus of the map function |dz/dZ| , between the physical plane and the halfplane, now occurs in the equations of motion in the Z-plane. (The compressible equations and boundary conditions are given in Appendix B.) So the wake shape must again be determined as part of the calculation, not only for the map itself but also for the flow in the Z-plane, and in applying the conditions on pressure and shape across it we cannot definitely appeal to formulae such as (2-12a, b) to relate slopes and velocities, since these are essentially incompressible results only. The revision of the wake shape, then, would seem to be the most troublesome aspect here although the flow equations are quite straightforward. It may be however that the incompressible shape would provide a good starting point and that another, intuitive, scheme of converging to the required shape can be devised even without explicit results such as (2-12b).

Work is currently in progress on extending the method, firstly to predict the effects of a trailing jet, secondly to include a turbulent boundary layer calculation, and thirdly to solve the compressible problem.

Acknowledgment

The author is very grateful to Professor K.W. Mangler for all his help and advice during this work, which was for the most part carried out in the Theoretical Aerodynamics Unit at Southampton.

Appendix A

SOME ASPECTS OF THE MAP FOR INCOMPRESSIBLE FLOWS

For incompressible motions, the profile produces disturbances just like those of a circle (*cf.* Sells[2], for example) as $|z| \to \infty$, so that

$$F \sim Ue^{-i\alpha}z + \frac{\Gamma i}{2\pi} \ln z + (\text{constant}) + o(1) \qquad \text{as} \quad |z| \to \infty \ . \tag{A-1}$$

On the other hand, F is known exactly in the Z-plane, by equation (2-5), and so, on equating (A-1) and (2-5) and expanding asymptotically, we find

$$\frac{dz}{dZ} \sim \left(\frac{AZ + B}{U}\right)e^{i\alpha}\left\{1 - \frac{\Gamma i}{\pi AZ^2} + o(Z^{-2})\right\} \ . \tag{A-2}$$

Along the wake $Z = X > 0$, $\theta \to \alpha$ and hence, since $\phi(X) = \theta(X)$ and $h \pm i\phi = \ln (dz/dZ)$,

$$\left.\begin{aligned} \theta(X) &= \phi(X) \sim \alpha - \frac{\Gamma}{\pi AX^2} + o(X^{-2}) \\ h(X) &\sim \ln\left(\frac{AX + B}{U}\right) + o(X^{-2}) \end{aligned}\right\} \tag{A-3}$$

as $X \to \infty$, and similarly for $X \to -\infty$. The decay of $H(X)$ in (2-14) then follows from (2-13a).

Further, the circulation Γ is equal to the jump in the velocity potential χ across the wake. But from (2-5)

$$\chi = \mathrm{Re}(F(Z)) = \tfrac{1}{2}AX^2 + BX$$

along the wake, $Y = 0$. Taking the jump at the wake points $X = \pm 1$, therefore

$$\Gamma = \chi(1) - \chi(-1) = 2B \ . \tag{A-4}$$

Appendix B

THE GOVERNING EQUATIONS IN THE Z-PLANE FOR COMPRESSIBLE FLOWS

First we express the equations of compressible motion in terms of the velocity potential χ, starting from the following equations, holding in the physical plane, for the velocity field $(u,v) = \underset{\sim}{\nabla}\chi$ (*cf.* Garabedian and Korn[3]):

$$\left.\begin{aligned} (a^2 - u^2)\frac{\partial u}{\partial x} - uv\left(\frac{\partial u}{\partial y} + \frac{\partial v}{\partial x}\right) + (a^2 - v^2)\frac{\partial v}{\partial y} &= 0 \\ \tfrac{1}{2}q^2 + \frac{a^2}{\gamma - 1} &= \tfrac{1}{2} + \frac{1}{(\gamma - 1)M_\infty^2} \end{aligned}\right\} \qquad \text{(B-1)}$$

where $q = (u^2 + v^2)^{\frac{1}{2}}$ is the flowspeed, a is the local speed of sound, and the freestream has Mach number $M_\infty < 1$ and unit speed. Transforming to the X, Y coordinates of the Z-plane and denoting $f \equiv |dz/dZ|$, (B-1) yields

$$\left.\begin{aligned} \chi_{XX}\left(a^2 - \frac{\chi_X^2}{f^2}\right) - 2\chi_X\chi_Y\frac{\chi_{XY}}{f^2} + \chi_{YY}\left(a^2 - \frac{\chi_Y^2}{f^2}\right) + \left(\frac{\chi_X^2 + \chi_Y^2}{f^3}\right)(\chi_X f_X + \chi_Y f_Y) &= 0 \\ q^2 = \frac{\chi_X^2 + \chi_Y^2}{f^2} & \end{aligned}\right\} \qquad \text{(B-2)}$$

as the equations of motion in the Z-plane.

Secondly, using the alternative governing equations

$$\left.\begin{aligned} \frac{\partial}{\partial x}(\rho u) + \frac{\partial}{\partial y}(\rho v) &= 0 \\ \frac{\partial v}{\partial x} - \frac{\partial u}{\partial y} &= 0 \end{aligned}\right\} \qquad \text{(B-3)}$$

produces (*cf.* Sells[2])

and

$$\left.\begin{aligned} \left(\frac{1}{\rho}\psi_X\right)_X + \left(\frac{1}{\rho}\psi_Y\right)_Y &= 0 \\ \frac{\rho^{\gamma-1}}{(\gamma - 1)M_\infty^2} + \left(\frac{\psi_X^2 + \psi_Y^2}{2\rho^2 f^2}\right) &= \frac{1}{(\gamma - 1)M_\infty^2} + \frac{1}{2} \end{aligned}\right\} \qquad \text{(B-4)}$$

in the X, Y coordinates, where the stream function ψ is defined by

$$\rho f u = \frac{\partial \psi}{\partial Y}, \quad \rho f v = -\frac{\partial \psi}{\partial X} \tag{B-5}$$

and ρ is the density, so that $q^2 = \left(\psi_X^2 + \psi_Y^2\right)\rho^{-2} f^{-2}$.

Solving (B-4) for the stream function ψ and density ρ would be equivalent to Sells[2] treatment of the subcritical problem using the circle transformation, while (B-2) for the velocity potential χ corresponds to the equations solved by Garabedian and Korn[3] for transonic calculations. The behaviour of χ, ψ, ρ and f at infinity, required to eliminate the singularities there, can be worked out by systematically expanding about the incompressible farfield (Appendix A) and it is found that, if $R^2 = X^2 + Y^2$,

$$\chi \sim \tfrac{1}{2}AR^2 \cos 2\Theta + BR \cos \Theta - \frac{\Gamma}{\pi}\left(1 - M_\infty^2\right)^{\frac{1}{2}} \left\{ -\Theta + \frac{\tan^{-1}\left[\left(1 - M_\infty^2\right)^{\frac{1}{2}} \tan 2\Theta\right]}{2\left(1 - M_\infty^2\right)^{\frac{1}{2}}} \right\}$$

$$\psi \sim \tfrac{1}{2}AR^2 \sin 2\Theta + BR \sin \Theta + \frac{\Gamma}{4\pi}\left(1 - M_\infty^2\right)^{\frac{1}{2}} \ln\left(1 - M_\infty^2 \sin^2 2\Theta\right)$$

$$f^2 \sim A^2R^2 + 2ABR \cos \Theta + B^2 - \frac{2A\Gamma}{\pi}\left(1 - M_\infty^2\right)^{\frac{1}{2}} \sin 2\Theta$$

$$\rho \sim 1 - \frac{\Gamma\left(1 - M_\infty^2\right) \sin 2\Theta}{\pi AR^2\left(\frac{1}{M_\infty^2} - \sin^2 2\Theta\right)}$$

as $R \to \infty$, where $\Theta = \tan^{-1}(Y/X)$. These agree with (A-1) for $M_\infty = 0$. The other boundary conditions, on the body and wake, are $\frac{\partial \chi}{\partial Y} = \psi = 0$ along $Y = 0$ in the halfplane, with appropriate discontinuity constraints across the wake ($|X| > 1$) .

SYMBOLS

A	unknown stretching-factor, equations (2-5) and (3-6)
B	unknown circulation-factor, equations (2-5) and (2-16)
d	trailing-edge angle
d_1, d_2	trailing streamline angles, Fig.2
F	complex potential
$\hat{f}$	scale factor, equation (3-6)
h	$\mathrm{Re}[\ln (dz/dZ)]$
H	well-balanced function related to k, equations (2-11) and (2-13)
I	integral in (3-4)
q	flowspeed
R	X_M
s	distance along aerofoil section
s_0	half the total arclength of the aerofoil
U	freestream speed
x, y	aerofoil coordinates in cartesian axes
X, Y	coordinates in the transformed plane
z, Z	$z = x + iy$, $Z = X + iY$
α	angle of incidence
Γ	circulation (= 4B)
Δ	constant steplength along X-axis
ε_1, ε_2	small displacements below $Z = \pm 1$
θ	flow inclination
ϕ, Φ	$\mathrm{Im}[\ln (dz/dZ)]$ and related function (see (2-11) and (2-13)), respectively

Affices

c	values in the Z-plane
i	values at $X = X_i$, $i = 1$ to M
J,N,K,M	values of i at $X = -1, 0, 1$ and at R, the end-point, respectively
$\hat{}$	values on the rigid body
$\pm$	upper and lower wake surfaces

REFERENCES

No.	Author	Title, etc.
1	D. Catherall D.N. Foster C.C.L. Sells	Twodimensional incompressible flow past a lifting aerofoil. RAE Technical Report 69118 (1969)
2	C.C.L. Sells	Plane subcritical flow past a lifting aerofoil. Proc. Roy. Soc. A 308, 377-401 (1968)
3	P.R. Garabedian D.G. Korn	Analysis of transonic airfoils. Comm. Pure Appl. Maths. 24, 841-851 (1971)
4	J.J. Kacprzynski L.H. Ohman P.R. Garabedian D.G. Korn	Analysis of the flow past a shockless lifting airfoil in-design and off-design conditions. NRC of Canada Aeron. Report LR-554, Ottawa (1971)
5	F. Bauer P.R. Garabedian D.G. Korn	A theory of supercritical wing sections, with computer programs and examples. Lec. notes in Economics and Math. Systems (Springer-Verlag, 1972)
6	D.G. Korn	Computation of shock-free transonic flows for airfoil design. Report NYU-NYO-1480-125 (1969)
7	D.N. Foster	Note on methods of calculating the pressure distribution over the surface of two-dimensional cambered wings. RAE Technical Report 67095 (1967)
8	A.M.O. Smith J.L. Hess	Calculation of potential flow about arbitrary bodies. Progress in Aeron. Sciences, Vol.8, Pergamon Press (1966)
9	B. Thwaites	On the numerical calculation of Theodorsen's transformation. ARC CP 691 (1963)
10	T. Theodorsen	Theory of wing sections of arbitrary shape. NACA Report 411 (1931)
11	E.M. Murman J.D. Cole	Calculation of plane steady transonic flows. AIAA Jnl. 9, 114-121 (1971)

REFERENCES (concluded)

No.	Author	Title, etc.
12	J.L. Steger H. Lomax	Numerical calculation of transonic flow about two-dimensional airfoils by relaxation procedures. AIAA 4th Fluid and Plasma Dynamics Conference, Palo Alto, Calif., (June 1971)
13	P.R. Garabedian D.G. Korn	Numerical design of transonic airfoils. Numerical solution of partial differential equations - II. Academic Press, New York, 253-271 (1971)
14	P.R. Garabedian D.G. Korn	Numerical design of transonic airfoils. Actes du Congrès International des Mathematiciens, 3, 95-97 (1971)
15	M.C.P. Firmin	Calculation of the pressure distribution, lift and drag on aerofoils at subcritical conditions. RAE Technical Report 72235 (1973)
16	B.J. Powell	The calculation of the pressure distribution on a thick cambered aerofoil at subsonic speeds including the effect of the boundary layer. ARC CP 1065 (1967)
17	G.F. Carrier M. Krook C.E. Pearson	Functions of a complex variable; theory and technique. Published by McGraw-Hill (1966)
18	J.M. Freeland	Cubic spline fitting. RAE Maths. Computing Note C335 (1965)

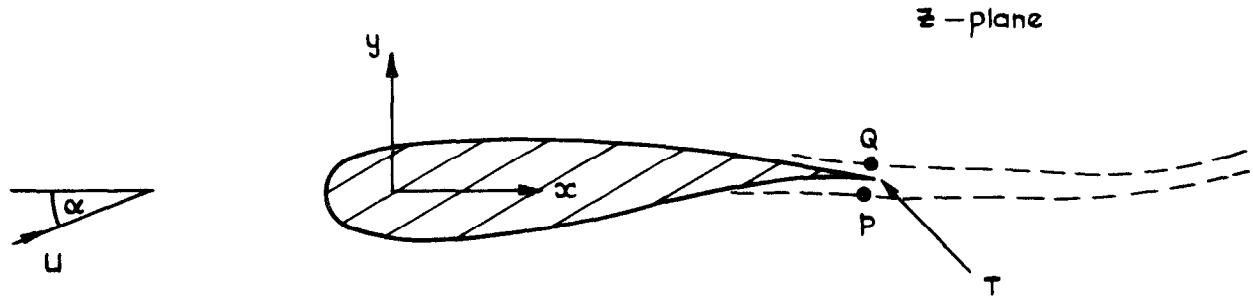

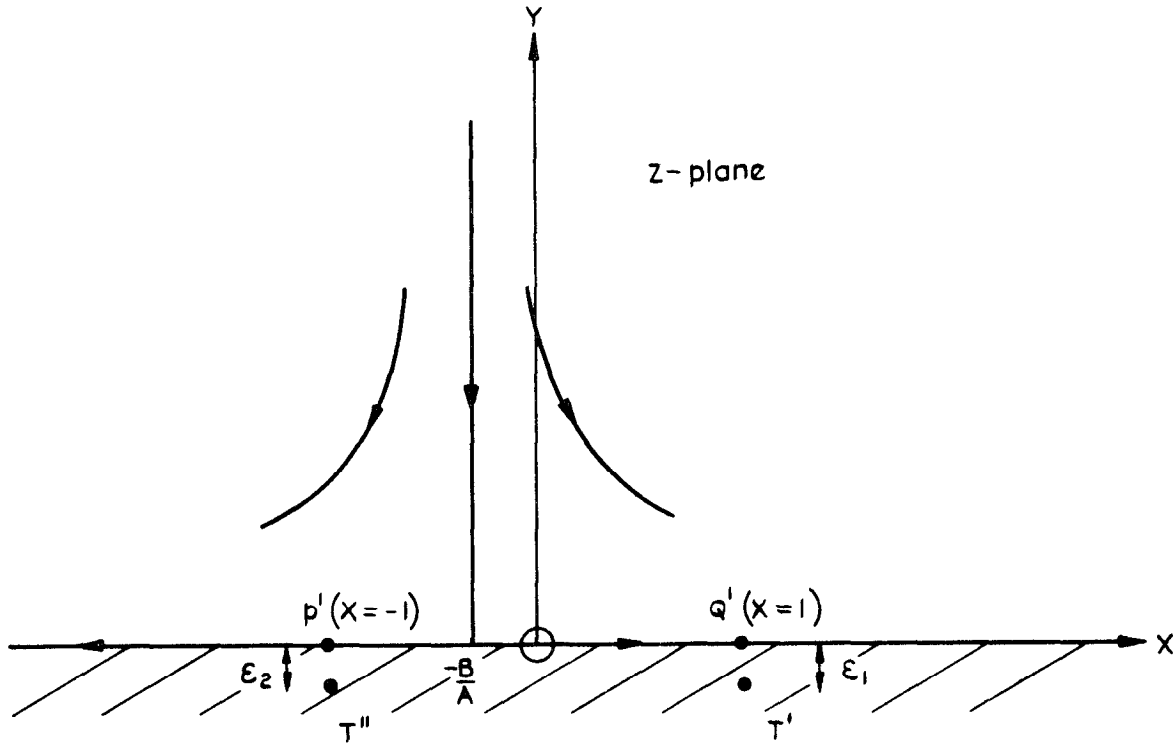

Fig.1 The map of the flowfield ($\mathbf{z}$) to the upper halfplane (Z)

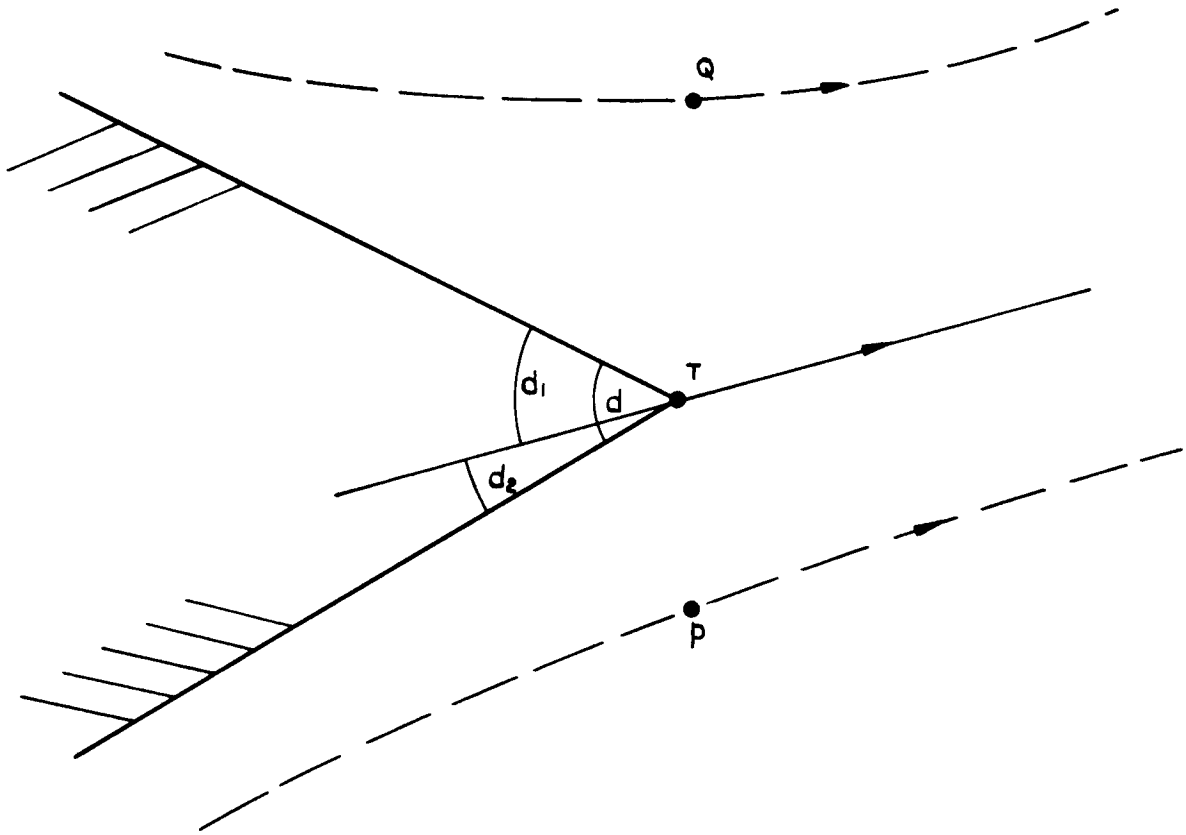

Fig. 2 The flow near the trailing-edge point T

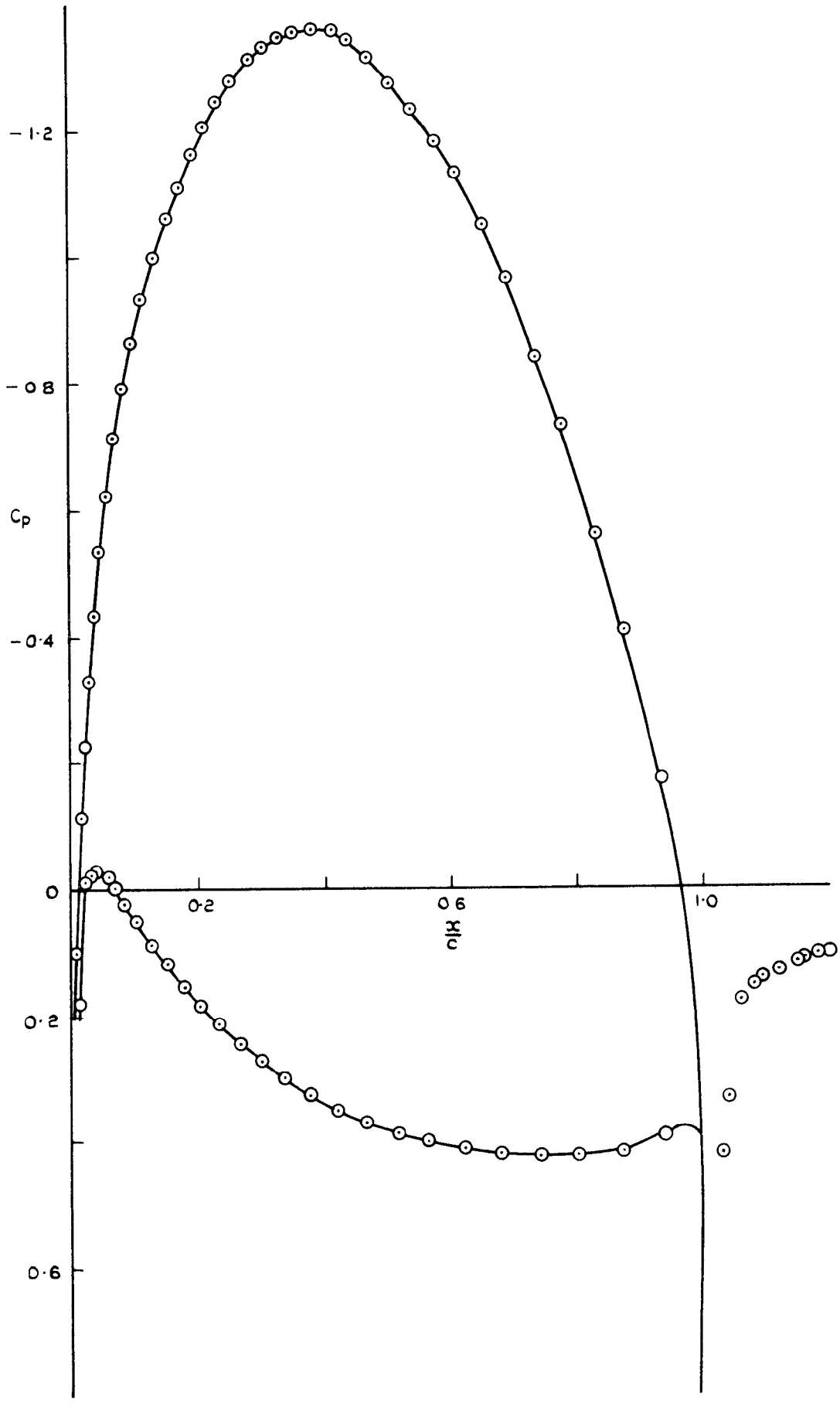

Fig. 3a The exact — and calculated ⊙ pressure coefficients for the medium – camber Karman – Trefftz profile, at $\alpha = 0°$ and with $\varepsilon_1 = \varepsilon_2 = 0$

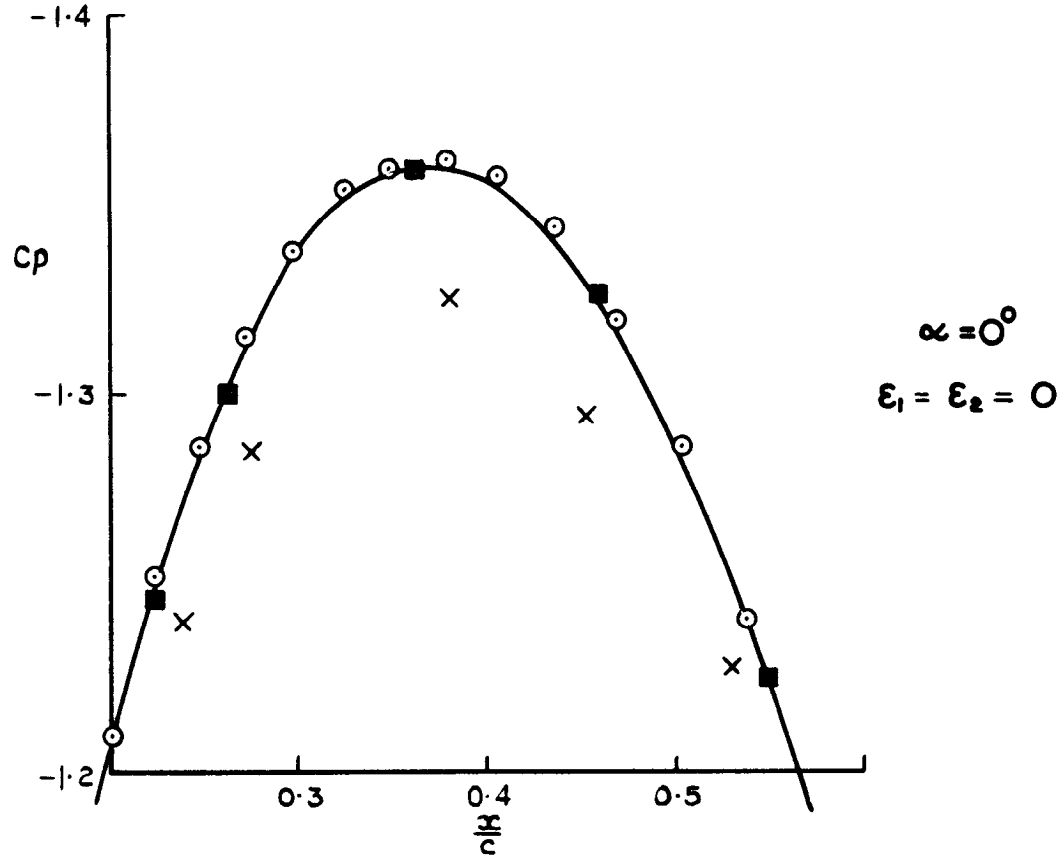

Fig 3b Results due to:- ⊙ present method, ■ Catherall et al[1] × AMO Smith[8] with 72 profile points

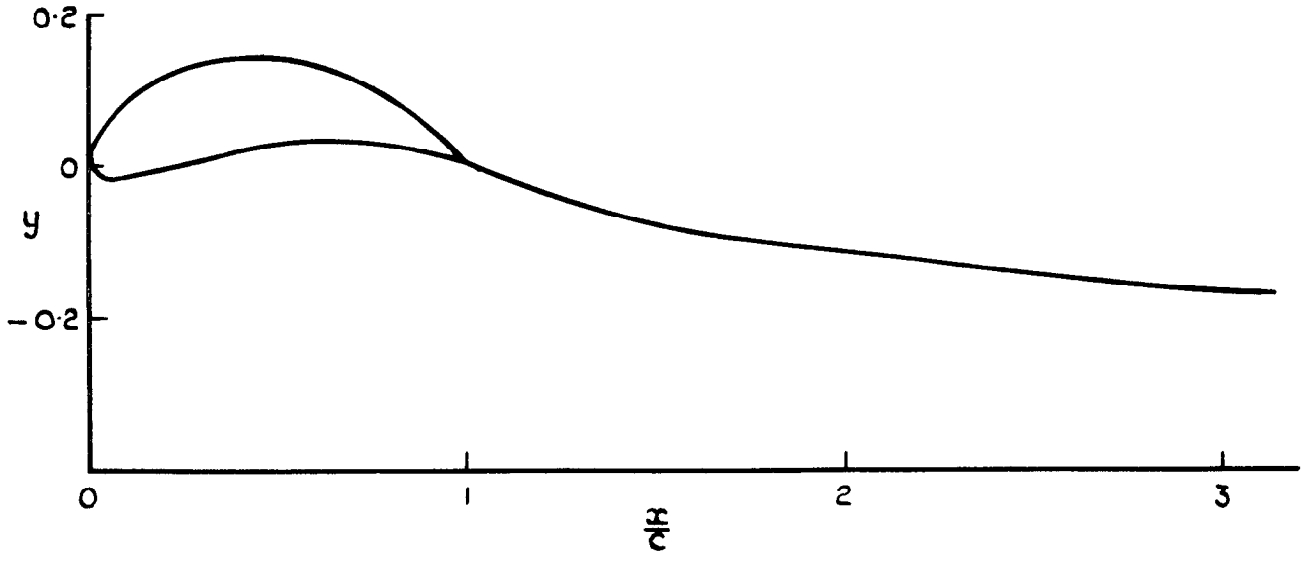

Fig. 3c The body and wake shape for $\alpha = 0^{\circ}$, $\varepsilon_1 = \varepsilon_2 = 0$

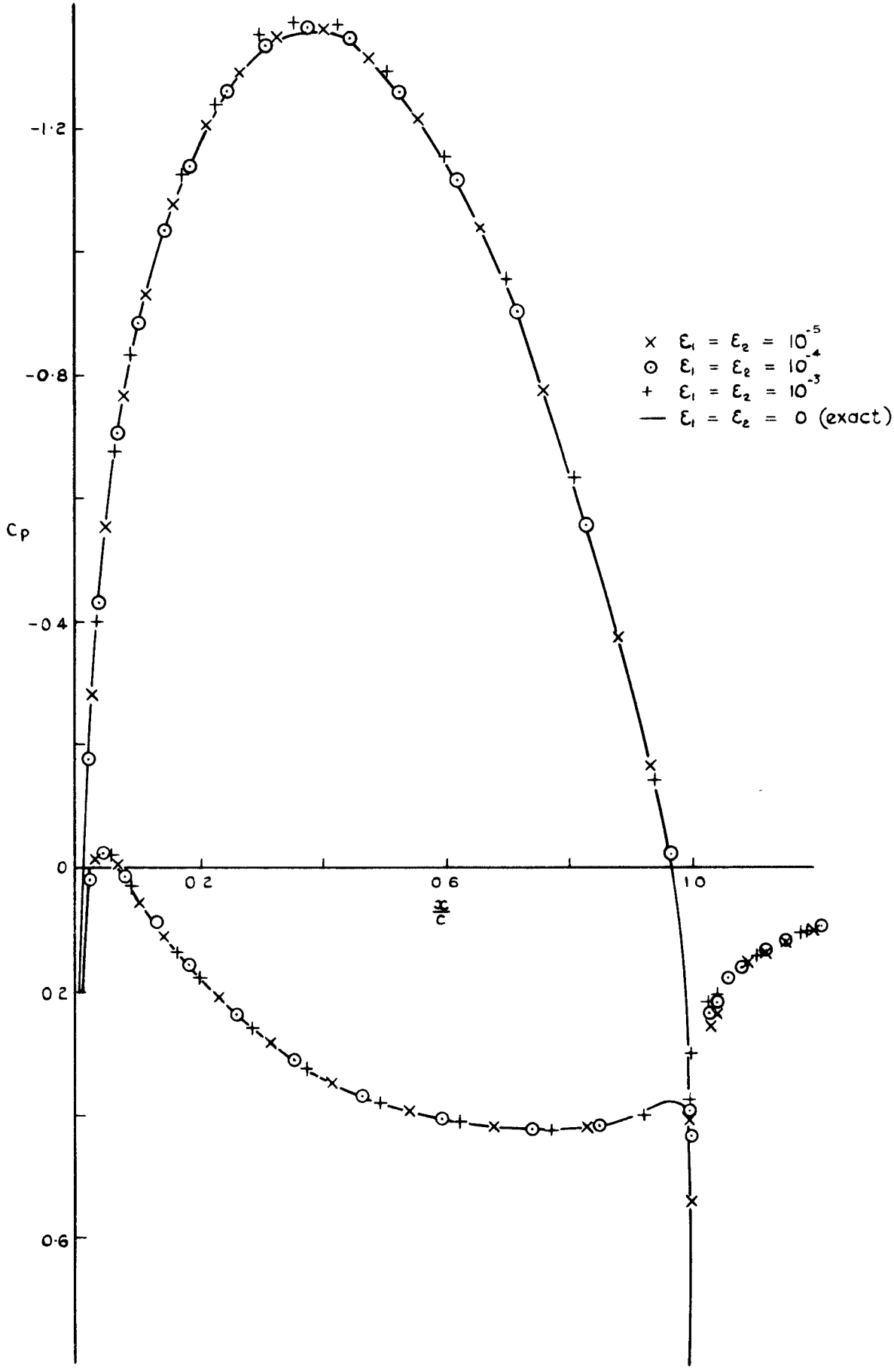

Fig. 4a Exact (for $\varepsilon_i = 0$) and calculated (for non zero ε_1) pressures at $\alpha = 0^\circ$

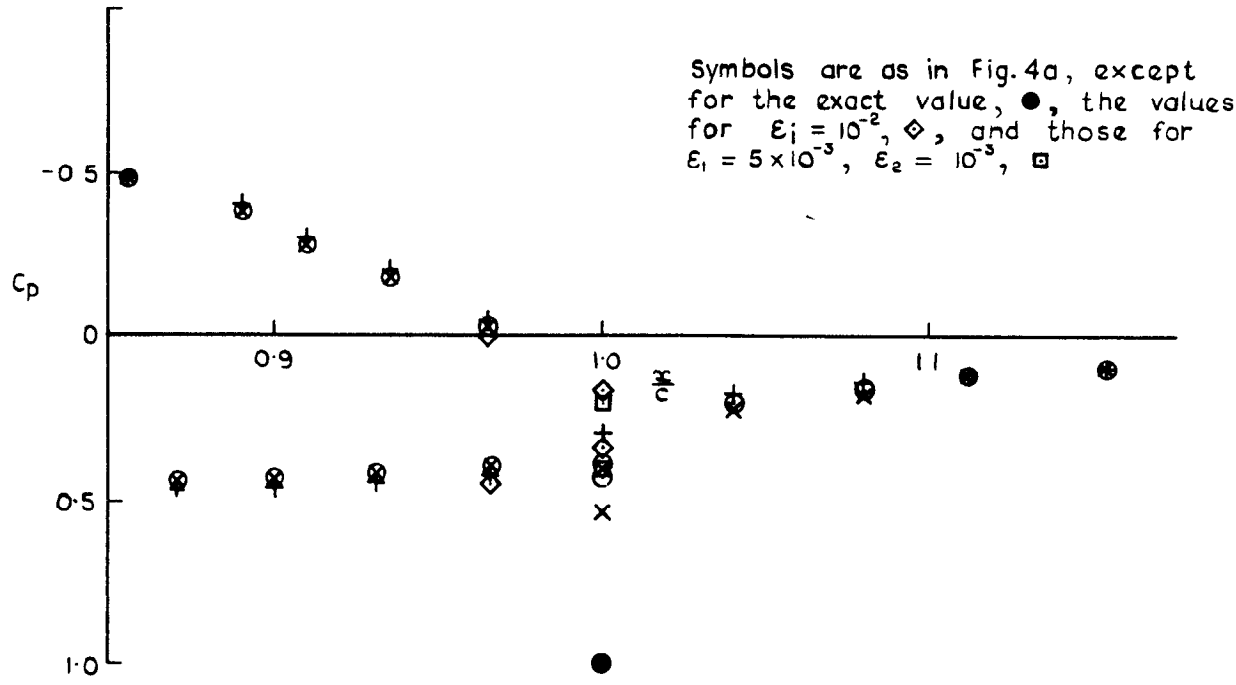

Fig. 4b Details of the pressure distribution near the trailing edge

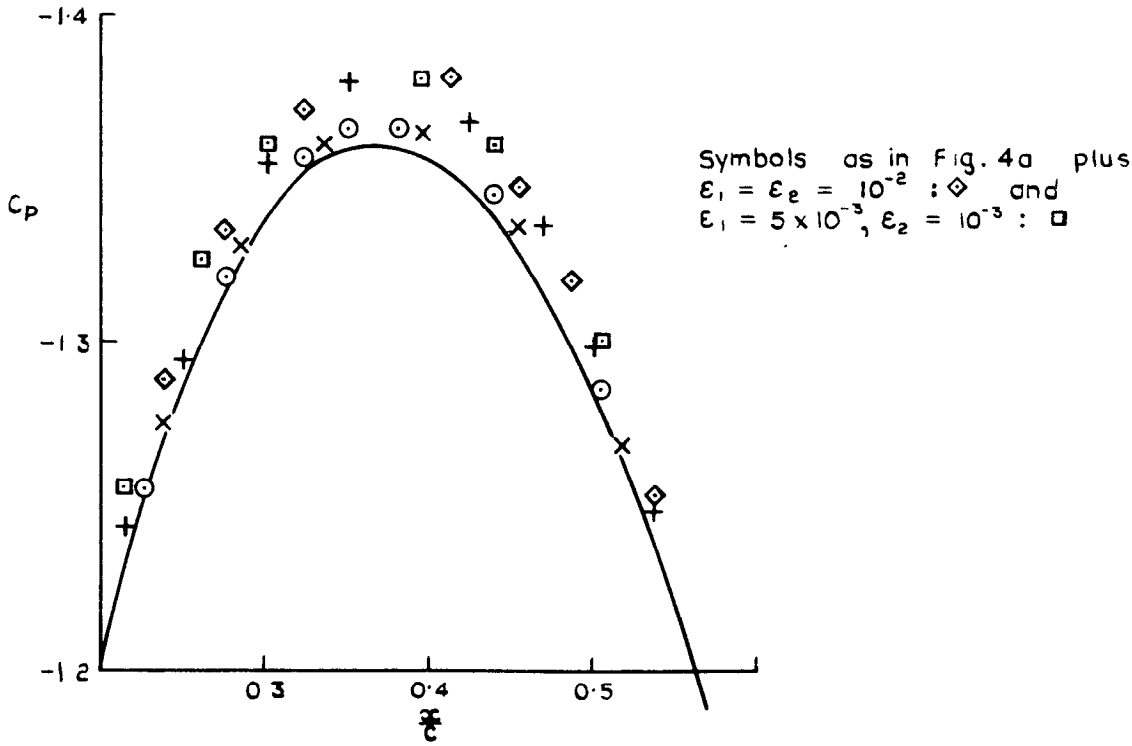

Fig. 4c The upper surface peak for non zero ε_1, ε_2 at $\alpha = 0^\circ$

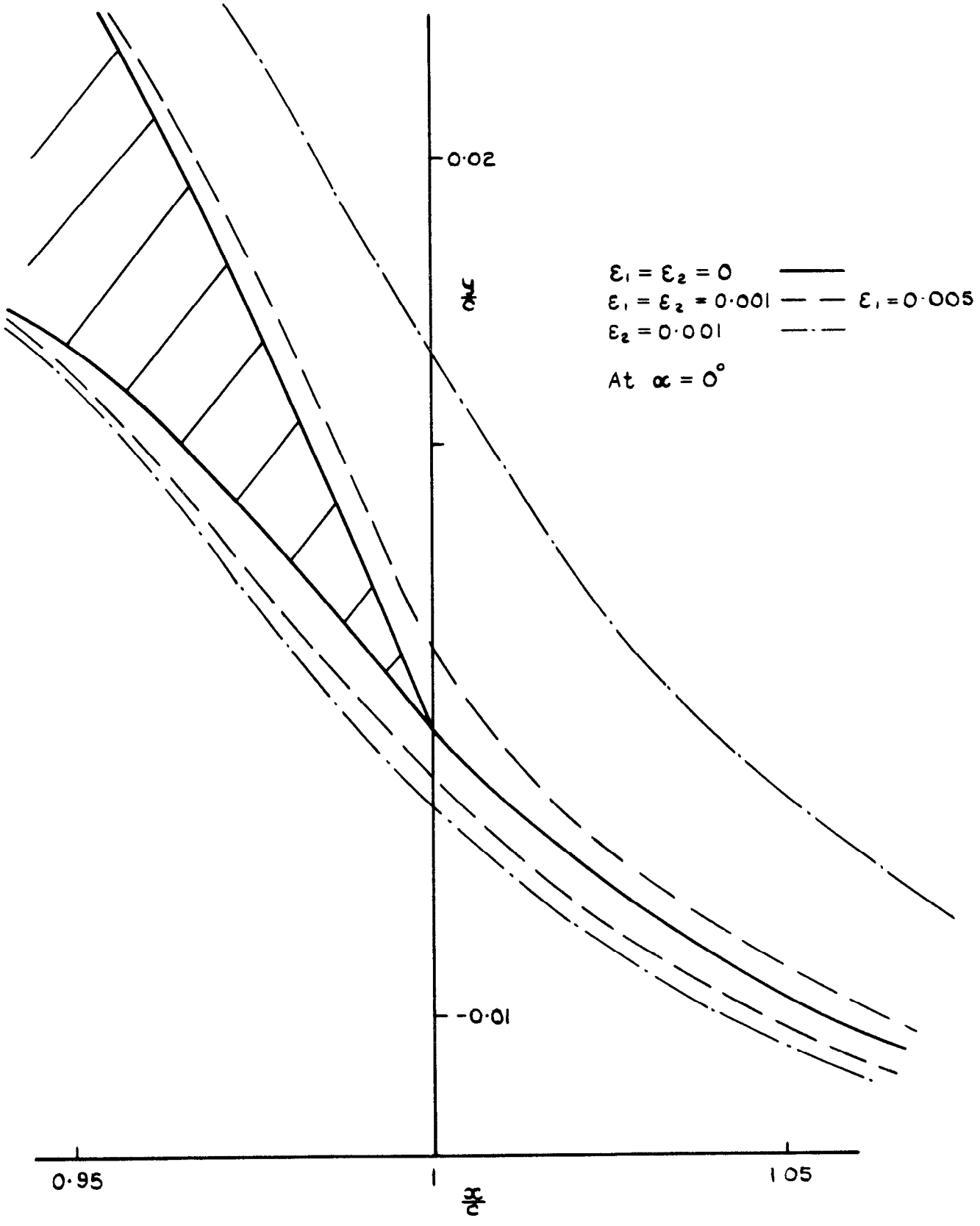

Fig. 4d Sketch of the body and wake shapes near the trailing edge

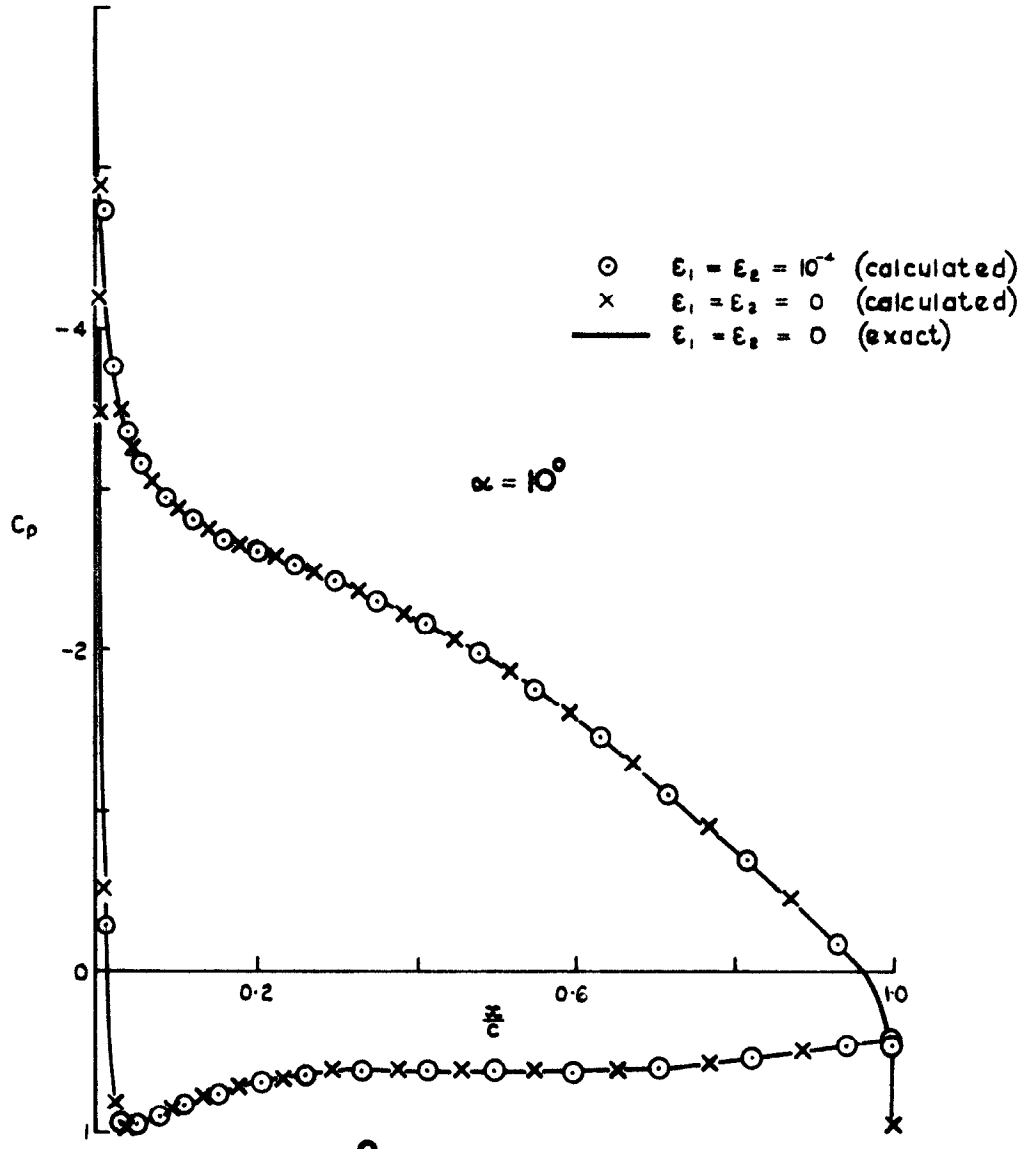

Fig. 5a For 10° incidence, the exact and calculated pressure coefficients

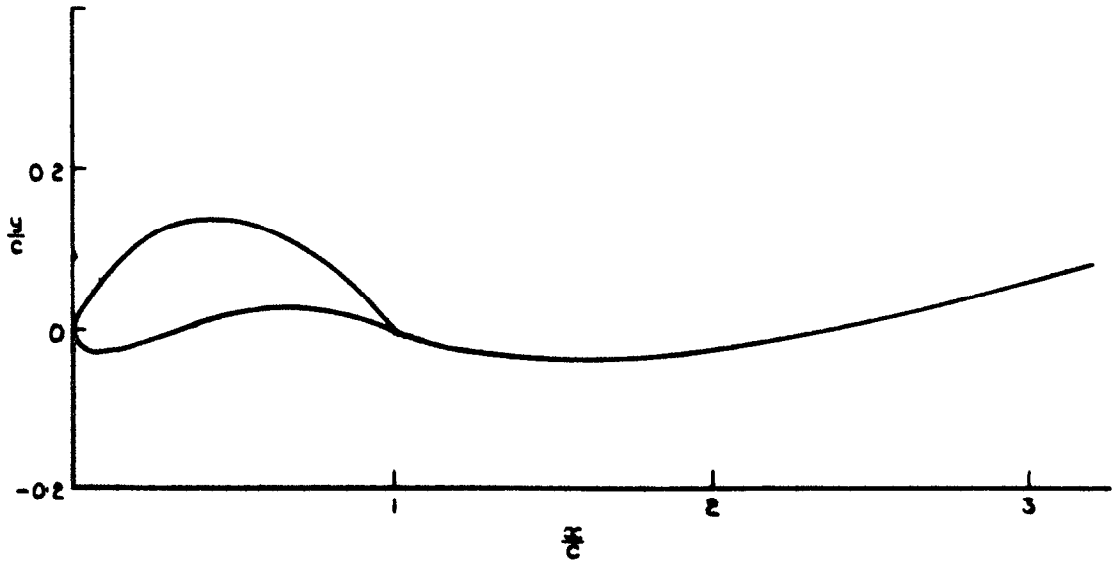

Fig. 5b The body and wake shape for $\alpha = 10^\circ$

Printed in England for Her Majesty's Stationery Office by the Royal Aircraft Establishment, Farnborough Dd 290279 K 5 9/76

ARC CP No 1352
November 1974

Smith, F T

533.6 011.32
533 692 :
533.6 048 3 .
532 526

PLANAR INCOMPRESSIBLE FLOW OVER AN AEROFOIL AND ITS WAKE

The Report describes a method for obtaining the incompressible flow over a given two-dimensional aerofoil at incidence, in which the rigid body and its boundary layer and wake are considered as forming a single semi-infinite body past which the inviscid fluid flows. The objective is to enable the viscous effects to be accommodated directly into an inviscid calculation, particularly near the sharp trailing-edge, where the singular point is in reality smoothed over by the boundary layer, and in the thin wake, whose shape has to be determined. By a conformal mapping to a halfplane an iterative cycle is set up to compute the solution, each iteration starting with a given shape, from which velocities are found, and ending with a suitable new guess for the wake shape, subject to certain conditions on the pressure and slope discontinuities across the wake Results are presented for a Karman-Trefftz section of medium camber, both in the inviscid limit of zero displacement thickness (in which there is very good agreement with the exact solution) and for small non-zero displacement thicknesses near the trailing edge and in the wake The method should be applicable to further problems.

ARC CP No.1352
November 1974

Smith, F. T.

533.6.011.32
533.692 .
533.6.048.3
532.526

PLANAR INCOMPRESSIBLE FLOW OVER AN AEROFOIL AND ITS WAKE

The Report describes a method for obtaining the incompressible flow over a given two-dimensional aerofoil at incidence, in which the rigid body and its boundary layer and wake are considered as forming a single semi-infinite body past which the inviscid fluid flows. The objective is to enable the viscous effects to be accommodated directly into an inviscid calculation, particularly near the sharp trailing-edge, where the singular point is in reality smoothed over by the boundary layer, and in the thin wake, whose shape has to be determined By a conformal mapping to a halfplane an iterative cycle is set up to compute the solution, each iteration starting with a given shape, from which velocities are found, and ending with a suitable new guess for the wake shape, subject to certain conditions on the pressure and slope discontinuities across the wake. Results are presented for a Karman-Trefftz section of medium camber, both in the inviscid limit of zero displacement thickness (in which there is very good agreement with the exact solution) and for small non-zero displacement thicknesses near the trailing edge and in the wake. The method should be applicable to further problems.

DETACHABLE ABSTRACT CARDS

ARC CP No.1352
November 1974

Smith, F. T.

533.6.011 32
533.692
533 6.048 3
532 526

PLANAR INCOMPRESSIBLE FLOW OVER AN AEROFOIL AND ITS WAKE

The Report describes a method for obtaining the incompressible flow over a given two-dimensional aerofoil at incidence, in which the rigid body and its boundary layer and wake are considered as forming a single semi-infinite body past which the inviscid fluid flows The objective is to enable the viscous effects to be accommodated directly into an inviscid calculation, particularly near the sharp trailing-edge, where the singular point is in reality smoothed over by the boundary layer, and in the thin wake, whose shape has to be determined. By a conformal mapping to a halfplane an iterative cycle is set up to compute the solution, each iteration starting with a given shape, from which velocities are found, and ending with a suitable new guess for the wake shape, subject to certain conditions on the pressure and slope discontinuities across the wake Results are presented for a Karman-Trefftz section of medium camber, both in the inviscid limit of zero displacement thickness (in which there is very good agreement with the exact solution) and for small non-zero displacement thicknesses near the trailing edge and in the wake The method should be applicable to further problems.

Cut here

ARC CP No 1352
November 1974

Smith, F T.

533 6.011.32
533 692
533 6 048.3 ·
532 526

PLANAR INCOMPRESSIBLE FLOW OVER AN AEROFOIL AND ITS WAKE

The Report describes a method for obtaining the incompressible flow over a given two-dimensional aerofoil at incidence, in which the rigid body and its boundary layer and wake are considered as forming a single semi-infinite body past which the inviscid fluid flows The objective is to enable the viscous effects to be accommodated directly into an inviscid calculation, particularly near the sharp trailing-edge, where the singular point is in reality smoothed over by the boundary layer, and in the thin wake, whose shape has to be determined. By a conformal mapping to a halfplane an iterative cycle is set up to compute the solution, each iteration starting with a given shape, from which velocities are found, and ending with a suitable new guess for the wake shape, subject to certain conditions on the pressure and slope discontinuities across the wake Results are presented for a Karman-Trefftz section of medium camber, both in the inviscid limit of zero displacement thickness (in which there is very good agreement with the exact solution) and for small non-zero displacement thicknesses near the trailing edge and in the wake. The method should be applicable to further problems.

Cut here

DETACHABLE ABSTRACT CARDS

Published by
HER MAJESTY'S STATIONERY OFFICE

Government Bookshops
49 High Holborn, London WC1V 6HB
13a Castle Street, Edinburgh EH2 3AR
41 The Hayes, Cardiff CF1 1JW
Brazennose Street, Manchester M60 8AS
Southey House, Wine Street, Bristol BS1 2BQ
258 Broad Street, Birmingham B1 2HE
80 Chichester Street, Belfast BT1 4JY
Government Publications are also available through booksellers

C.P. No. 1352

ISBN 011 470988 2